Study of the sector structure in adularia by means of optical microscopy, infra-red absorption, and electron microscopy

MIZUHIKO AKIZUKI AND ICHIRO SUNAGAWA

Institute of Mineralogy, Petrology, and Economic Geology, Faculty of Science,
Tohoku University, Sendai. 980, Japan

SUMMARY. Surface microtopography of habit faces, and internal textures of corresponding growth sectors of adularia from the Rhonegletscher, Switzerland, and the Seikoshi mine, Japan, were studied by means of optical polarizing microscopy, reflection interference contrast, electron microscopy, and infra-red absorption spectroscopy. Thin sections parallel to the growth plane were prepared from the specimen whose as-grown face was pasted on a glass slide. Most internal textures seen optically in the thin sections correlated well with the growth patterns for both specimens (fig. 1). Thin foils prepared by ion-thinning from the Rhonegletscher adularia show, under the electron microscope, coexisting heavily cross-hatched areas giving diffuse diffraction spots and homogeneous areas giving sharp diffraction spots. As a whole, adularia from the Seikoshi mine gives more homogeneous and much weaker cross-hatching than the Rhonegletscher specimens. Also, infra-red absorption spectra, which correlate very well with the Al/Si ordering and the optics, show that the {110} growth sector consists of triclinic disordered K-feldspar and the {001} and {101} sectors monoclinic high or low sanidine or orthoclase.

These observations indicate that the characteristic internal textures seen on all optical micrographs are formed during the process of crystal growth, and are not due to monoclinic-triclinic transition. Although the transition process has taken place to a slight extent, the original growth textures remain well preserved throughout geological time. It is suggested from these observations that the degree of Al/Si ordering is mainly controlled by the different rates of growth and the different two-dimensional atomic arrangements exposed on the various growth surfaces. The higher the growth rate the more disordered are the phases that form. The symmetry of the two-dimensional atomic arrangement is kept during growth regardless of the degree of ordering; {001} and {101} growth sectors whose crystal surfaces are parallel to b-axis are monoclinic, and the {110} sector whose surface is inclined to the b-axis is triclinic.

ADULARIA, a low-temperature feldspar with composition $KAlSi_3O_8$, occurs in two main varieties, one transparent and occurring in Alpine

fissures to which the name adularia is usually applied, the other sub-transparent, occurring as a gangue mineral in hydrothermal ore deposits, called valencianite.

Mallard (1876) found that apparent single crystals of adularia were actually composed of a rhombic centre showing extinction parallel to (010) and four-sectored rims having extinction angles of 2–3° from (010). The (110) and ($\bar{1}\bar{1}$0) sectors showed simultaneous extinction in the positive direction and the ($\bar{1}$10) and (1$\bar{1}$0) sectors in the negative direction. The (110) and (1$\bar{1}$0) sectors were related by the albite twin law, as were the ($\bar{1}$10) and ($\bar{1}\bar{1}$0) sectors. Thus the 'core' is monoclinic and the 'rims' triclinic.

Barth (1928, 1929) described microcline-like cross-hatching in adularia crystals. Köhler (1928) measured extinction angles on a number of adularia crystals and suggested that adularia might have crystallized as a monoclinic phase and then transformed to microcline. Chaisson (1950) measured extinction angles, 2V, and the optic orientation of adularia crystals from several localities, and found that smaller crystals ($\simeq$ 1–2 mm) show, in general, wholly or nearly monoclinic optics, whereas crystals larger than 3 mm commonly showed extinction angles that increased towards the edges of the crystal. Chaisson also observed that the optic planes of the centres of some crystals were essentially normal to (010) whereas those of sectors near the edges were approximately parallel to (010). In going from monoclinic to triclinic adularia, the orientation of the optic plane changes to that of high sanidine rather than microcline. As the boundary plane separating the two sectors was not a common growth face in adularia, Chaisson thought that the textures were not formed during crystal growth.

Using X-ray methods, Laves (1950) studied thin sections of the same specimens described by

Chaisson. He found that the 'core' of the crystal was monoclinic ($\gamma^* = 90'' \pm 5'$) and that the 'rims' were distinctly triclinic.

Bambauer and Laves (1960) studied adularia from Val Casatscha, Switzerland, by optical and X-ray methods. In the same crystal there were portions showing essentially high sanidine optics (axial plane $\sim \|(010)$, $2V \simeq 50°$) and microcline optics (axial plane approximately $\perp$ (010), $2V \simeq 50°$). A continuous series of intermediate optical orientations was observed between these two extremes. The latter workers interpreted the observed optical textures in terms of original growth as sanidines and later transformation to microclines with different degrees of Al/Si order.

Ansilewski (1961) suggested that the texture originates in the process of crystal growth, because it is difficult to explain the optical properties and orientation by the transition from orthoclase to microcline. Also Steiner (1970) inferred from the geological evidence that the cooling rate of the adularia he studied was too great for the relationship to be explained by transition into microcline, and came to a similar conclusion.

Our opinion is that most previous workers had given too little attention to growth features in adularia. Therefore, we attempted in this study to correlate the optical properties, the internal textures, and the growth features observed on the surfaces of crystal faces of adularia from Alpine mineral fissures and valencianite from epithermal veins, so that the role of the growth process in Al/Si order-disorder may be re-examined.

Furthermore, the structure and texture were studied using infra-red absorption spectra, which are known to correlate well with the structural states of potassium feldspar (Hafner and Laves, 1957), and electron microscopic observation. McConnell (1965) proposed that the fine cross-hatching seen optically and under the electron microscope was due to the phase transition from monoclinic to triclinic symmetry.

We have published elsewhere (Akizuki and Sunagawa, 1975) a paper devoted almost entirely to optical observations. In the present paper the subject is treated as a whole including, for more easy reference, some of these optical observations.

Specimens. Studies were made of adularia crystals collected from Alpine mineral fissures at Rhonegletscher, Switzerland, and of valencianite crystals from epithermal Au-Ag-quartz veins at the Seikoshi mine, Shizuoka Pref., Japan.

The adularia crystals from Rhonegletscher, Switzerland, are 1–5 cm in length, and show stout prismatic habit consisting of m {110}, x {$\bar{1}$01}, and c {001} faces. Crystals are transparent, and their surfaces are flat, showing no evidence of split

growth, which is different from the specimen of the Seikoshi mine. Their compositions [$Or_{88.5}Ab_{10.5}An_{0.2}Cn_{0.8}$ (Cn refers to Celsian)] were obtained by means of wet chemical analysis. The specimen is non-perthitic, typical microclinic textures were not found optically, though a few weakly cross-hatched regions were seen around very small inclusions under the polarizing microscope.

The valencianite crystals from the Seikoshi mine occur in cavities and are the latest stage products of the veins, growing on quartz crystals. From the homogenization temperatures of two-phase inclusions in quartz crystals associated with valencianite, it is estimated that the valencianite crystals are formed at relatively low temperatures, probably between 160 C to 200 °C or less. The crystals are subtransparent and are 1 2 cm in length, showing stout prismatic habit consisting of m {110} and x {$\bar{1}$01} faces, the {001} face being absent. Their compositions are estimated to be $Or_{94.5}Ab_{5.0}An_{0.5}$, on the basis of a partial chemical analysis. The crystals are non-perthitic and chemically homogeneous within 1 % error by electron probe microanalysis.

Methods. The surface microtopographs of crystal faces were studied by means of a reflection-type interference contrast microscope, which can reveal growth steps of the order of 1 Å on the surface. Various forms of growth pyramids were seen on crystal faces, from the analysis of which one may conjecture the growth process of the crystal.

Special sections were prepared in some cases parallel to or perpendicular to the as-grown face so as to correlate growth features (surface microtopographs of crystal faces) with internal textures as well as with optical properties. These sections were observed under the polarizing microscope with the universal stage to measure 2V values and extinction angles. Sections parallel to (010), which is not a habit face, were also prepared to investigate internal textures. The crystals from both localities consist of sector type textures, which correspond to growth regions of each of the habit faces. Thus they are called in this paper sectors of {$\bar{1}$01}, {001}, {110}, and {010}, according to the corresponding growth faces.

Following optical microscopic investigation, each growth sector was separated from the thin sections, and was studied by means of infra-red absorption and transmission electron microscopy. The domains in each sector that correspond to individual growth hillocks were too small to be separated for infra-red study. Thin foils for electron microscopy were prepared by means of ion bombardment.

GROWTH FEATURES AND INTERNAL TEXTURES

Adularia from Rhonegletscher, Switzerland

Characteristics of the crystals are:

A large number of growth hillocks are seen on the surfaces of $\{\bar{1}01\}$, $\{001\}$, and $\{110\}$ faces, suggesting rapid growth at least at the latest stage of growth.

The crystal consists of a more or less optically homogeneous central portion and thin optically inhomogeneous rim portions. This shows an abrupt change of growth conditions at the latest stage of growth, which corresponds to the feature described above.

The crystal consists of four $\{110\}$ sectors, an $\{001\}$, and a $\{\bar{1}01\}$ sector. The $\{110\}$ sectors are optically triclinic and are in fourling twin relations, while both $\{001\}$ and $\{\bar{1}01\}$ sectors are principally monoclinic, and these are similar to those observed by Chaisson (1950).

The characteristics of each growth sector and habit face are described below in some detail:

$\{\bar{1}01\}$ sector. On the $(\bar{1}01)$ face, a few large growth pyramids about 1 mm in diameter and several hundred μm in thickness are seen to coexist. The large pyramids are in trapezoidal form, with monoclinic symmetry, the minute ones are rounded (fig. 1a). Population of the minute pyramids is $1 \times 10^5/\text{cm}^2$, which is abnormally high for natural crystals, and as high as for synthetic crystals, suggesting high growth rates at the latest stage of growth.
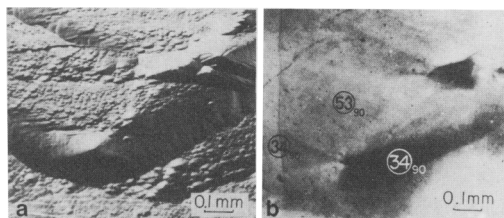

FIG. 1. Corresponding reflection interference-contrast (a) and polarized (b) micrographs of $(\bar{1}01)$. Rhonegletscher. The b-axis is horizontal. Numerals in circles show $2V_\alpha$ values and the suffixes the angles between the optic plane and (010).

A thin section parallel to the $\{\bar{1}01\}$ face was prepared from the specimen whose as-grown face was pasted on a slide glass. Fig. 1b shows a photomicrograph under crossed polars of the same area as in fig. 1a. Clear one-to-one correlation is seen between the two photographs, especially for the large growth pyramids. The large growth pyramid consists of four side faces. Under the polarizing microscope (fig. 1b), the area corresponding to the large growth pyramid is divided into four domains, which have different optic axial angles: two opposite wing-like domains showing $2V_\alpha$ 34° and optic plane nearly $\perp$ (010) whose extinction angles deviate 2° from (010), i.e. they are optically triclinic and are in the relation of albite twinning to each other, whereas the largest domain shows $2V_\alpha$ 53°, with the optic plane normal to (010), and is optically monoclinic, and the lower domain shows varying 2V values from 34° to 53° with the extinction angle changing gradually from 2° to 0° from (010). Although similar correlation may be found for smaller and rounded growth pyramids, the resolution of optical microscopy is too low to detect this. However, the average optics of the areas corresponding to minute growth pyramids are $2V_\alpha$ 53°, and optic plane $\perp$ (010). It should be noted here that this optical heterogeneity is seen only within the thin rim portion of the crystal (down to 0·05 mm depth from the surface) and that the inner portion is more or less optically homogeneous with 2V values from 60° to 62°, except that in some cases there appear bands parallel to b that have $2V_\alpha = 38\text{-}52°$.

$\{001\}$ sector. The (001) surface is covered by some large rhombic growth pyramids, which are less than about 1 cm in diameter and about 1 mm in thickness. The rhombic pyramids consist of narrowly spaced growth layers, and in some cases the layers are so narrowly spaced as to result in smooth-sided vicinal faces. The pyramids have pointed summits, suggesting that they were formed around line defects.

Under the microscope, the thin section prepared in a similar manner to that in the previous case shows rhombic domains that have one-to-one correlation with the growth pyramids on the surface, though the correlation is not as good as in the sectors of $\{\bar{1}01\}$ and $\{110\}$: the domains corresponding to large and thick growth pyramids are easily seen, but the domains corresponding to thinner layers are not clear. Since 2V values are not measurable on the (001) thin section, correlation was not established between the optical properties and growth features in this case. The inner portion is more or less optically homogeneous, with 2V values in the range of 20–30° and optic plane $\perp$ (010), though a few bands parallel to the b-axis develop in it.

$\{110\}$ sector. The $\{110\}$ faces are covered by many larger growth hillocks bounded by [001], [$\bar{1}$10], and [$1\bar{1}1$] directions, and they are less than several mm in diameter and less than about 1 mm in thickness.

In the [001] direction, the side vicinal faces consisting of steps of growth layers have steep slopes, whereas in the [$\bar{1}$10] and [1$\bar{1}$1] directions, they are gently inclined. These hillocks are composed of prismatic patterns elongated parallel to the c-axis (fig. 2a). The rhombic patterns bounded by [001] and [$\bar{1}$10] are formed by the pile of growth layers coming from a few growth centres. The thin section prepared from the specimen whose as-grown face was pasted on a slide glass shows that there is one-to-one correlation between growth hillocks and optical domains and that the area corresponding to the side vicinal faces has different optics from the central area (fig. 2b). The optics of the {110} sector are plotted in fig. 7A.
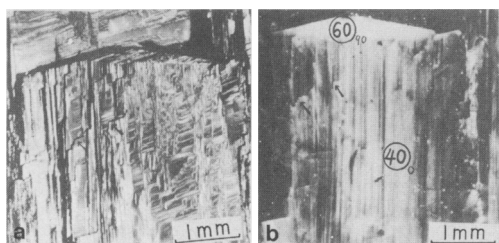

FIG. 2. Corresponding reflection interference-contrast (a) and polarized (b) photomicrographs of (110). Rhone-gletscher. Arrows show the corresponding positions. The c-axis is vertical.

Valencianite from the Seikoshi mine, Japan

A thin section normal to c-axis of this specimen shows that the crystal consists of {110}, {010}, and {$\bar{1}$01} sectors; within each sector finer textures are seen under the polarizing microscope (fig. 3). Areas m_1 and m_2 in fig. 3 are {110} sectors that are in albite twinning relation each other, and these are similar to those observed by Chaisson (1950). The {110} areas are composed of the lamellae parallel to {110}, and show different optical extinction angles from place to place. The area x in fig. 3 is the {$\bar{1}$01} sector and is composed of many rhombic patterns, which correspond to the growth hillocks on the {$\bar{1}$01} surface. The extinction angles within the rhombic pattern change gradually from place to place. The orientations of the areas b_1 and b_2, which are {010} sectors, are identical with those of the areas m_1 and m_2, respectively.

Oriented thin sections parallel to (110), (010), and ($\bar{1}$01) faces were prepared, and their optical properties were measured, along with a comparison with external forms of crystals and surface micro-topographs of (110) and ($\bar{1}$01) faces. Detailed descriptions of each sector are:

{$\bar{1}$01} sector. Most growth pyramids on the {$\bar{1}$01} face are rhombic in form, and are homologous with

the external outline of the face. They are less than about 3 mm in diameter and less than about 0·5 mm in thickness. They are in most cases pyramidal with pointed summits. Under the polarizing microscope, rhombic domains are seen in this section, and they show one-to-one correlation with the growth pyramids on the {$\bar{1}$01} surface, as in the case of the Alpine crystals.
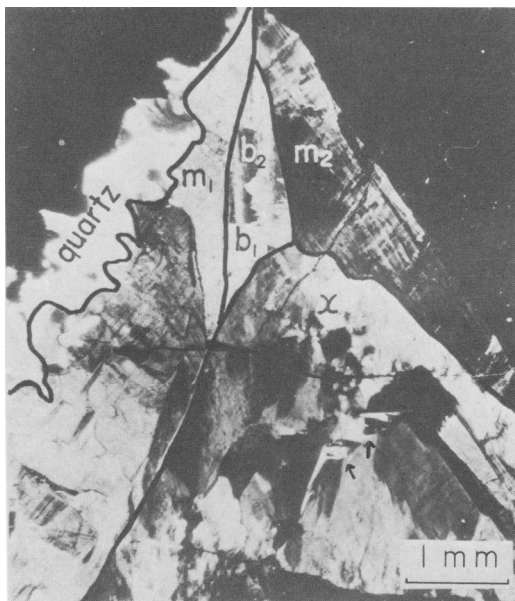

FIG. 3. Polarized optical photomicrograph of adularia from the Seikoshi mine showing growth sectors x, m, b in thin section (001). The b-axis is vertical.

The {$\bar{1}$01} sectors in the thin sections (110) are seen in the upper parts of fig. 4 in which fine growth lamellae are seen running parallel to the edges appearing at the upper portions of the figures, and these edges correspond to the growth face {$\bar{1}$01}. The area shows very wavy extinction. This is considered to be due to the split growth and to the fact that the growth hillocks on the {$\bar{1}$01} face contain both {110} and {010} domains.

The optic plane is normal or nearly normal to (010) in the area above the dotted line in fig. 4, and is parallel or nearly parallel to (010) below the line. The angle 2V decreases gradually with distance from the edge and becomes zero at the dotted line, and again increases gradually going inwards from the line, as can be seen from the values indicated in fig. 4. The optic angle and the orientation of optic plane measured on thin sections ($\bar{1}$01) and (110) are plotted in fig. 5. The arrows in fig. 5 show the change of optics during crystal growth.
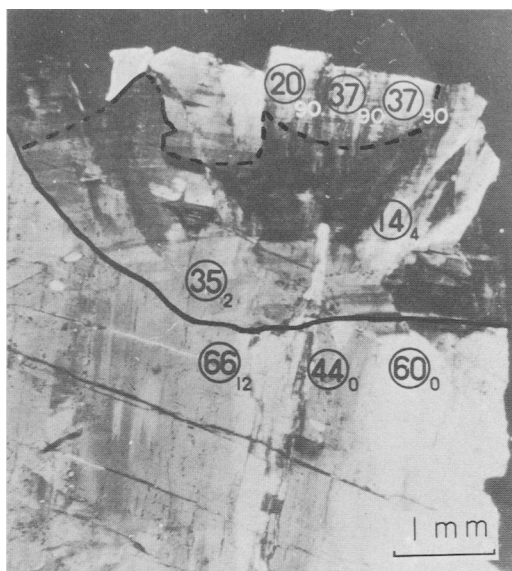
FIG. 4. Polarized photomicrograph showing the {110} and {$\bar{1}$01} sectors in thin section (110). Seikoshi mine. Numerals in circles show $2V_\alpha$ values and the suffixes the angles between the optic plane and (010). The c-axis is vertical.
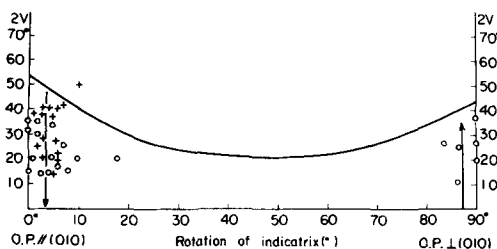

FIG. 5. Range of optical variations in the {$\bar{1}$01} and {010} sectors of adularia from the Seikoshi mine. The optics of {$\bar{1}$01} and {010} sectors are shown by open circle and cross, respectively. Curved line shows the optical variation in fig. 7. See the text for details.
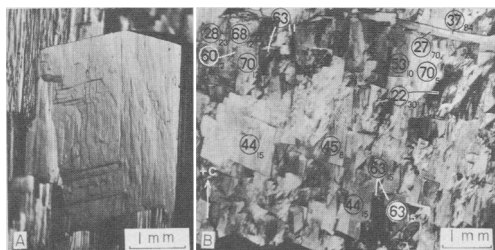

FIG. 6. Reflection interference-contrast photomicrograph of (110) surface (A), and polarized photomicrograph of (110) sector in thin section (110) (B). Seikoshi mine. Numerals in circle and suffixes are the same as in fig. 4.

{*010*} *sector.* The {010} faces are not seen as habit faces, but the sectors appear in the section (001). The {010} sectors marked b_1 and b_2 in fig. 3 gradually diminish in size with distance from the centre, i.e. as growth proceeds.

The orientations of the areas b_1 and b_2 in fig. 3 are identical with those of the areas m_1 and m_2 respectively, and both areas are in the relation of albite twinning. Similar relation is also seen in the individual small rhombic patterns in the ($\bar{1}$01) section, as indicated by arrows (fig. 3). The optic angle and the orientation of optic plane measured on the ($\bar{1}$01) thin section are plotted in fig. 5.

{*110*} *sector.* The {110} growth surfaces are characterized by the development of many stout prismatic, rhomboidal hillocks and striations parallel to c-axis (fig. 6A). The thin section parallel to (110) (fig. 6B) clearly shows that the crystal consists of a large number of rhomboidal domains. Although the photograph shown in fig. 6B resembles very much the surface microtopograph of the face, this is not the reflection photomicrograph of the surface but the micrograph (polarizing microscope) of a thin section both of whose surfaces are polished. Some domains consist of a central area surrounded by several strips; the central area corresponds to the area formed by the growth layers parallel to (110), and the strips to the portions formed by the pile-up of edges of growth layers from the (110) face, i.e. vicinal side faces on each growth hillock. For simplicity, these vicinal faces are indexed (100), (010), ($\bar{1}$01), (001), (11$\bar{1}$), and (121) respectively, as schematically shown in fig. 7. The {110} sectors in the thin section prepared normal to the c-axis are composed of the lamellae parallel to (110) (fig. 3), and show different optical extinction angles and axial angles from place to place.

The optic angles and the orientations of optic planes measured at various points in the section (110) are indicated in fig. 6B and plotted in fig. 7B. In most of the {110} sector the optic plane changes in varying degree around the α-axis of the indicatrix from the orientation parallel to (010), through the intermediate state, to the orientation normal to (010). This variation corresponds to the variation in the inclination of vicinal faces, as can be seen in fig. 7B. The area consisting of growth layers parallel to the growth face (110) has the optic orientation of high sanidine. The areas (010), (121), ($\bar{1}$01), etc., i.e. the areas corresponding to the vicinal side faces on the growth hillocks, have inclined optic planes. The greater the inclination of the side vicinal faces of growth hillocks, the more the optic plane is inclined, in a clockwise manner until it reaches to the position normal to (010). In general, therefore, 2V values plot on the curved line in fig. 7B. However,

FIG. 7. Variation in $2V_\alpha$ values and indicatrix rotation around α-axis within the $\{110\}$ sector. Figs. A and B are those of adularia from Rhonegletscher and the Seikoshi mine, respectively. Symbols show the position in each domain, and they correspond to the vicinal side faces on the growth hillocks. The symbols and the corresponding positions are schematically shown in the lower part of the figure. Although the portions surrounding the central area are indicated by low index faces, these are actually vicinal faces. Open circles of fig. A show the optics, which were measured on thin section roughly parallel to (1̄01). As the texture seen in such section is lamellae formed by stacking of the hillocks, the corresponding positions are not clear.

some deviate from the line; these are the values measured in the areas (100), (001), and (hkl). The reason for this deviation is not clear at present. In addition, there are two points, indicated by arrows in fig. 7B, that deviate from their expected positions, i.e. on the microcline side of the figure. These two values are measured on a well-developed (1̄21) face appearing on the side vicinal faces of growth hillocks on (110). Valencianite crystals from the Chitose mine, Hokkaido, Au–Ag-quartz veins, and from the Ani mine, Akita Prefecture, chalcopyrite-

pyrite–chlorite veins, were also studied for reference. Both growth features, internal textures, and optical properties were essentially similar to those observed in the crystals from the Seikoshi mine.

INFRA-RED ABSORPTION

Hafner and Laves (1957) made a detailed comparison of natural and synthetic K-feldspars using two well-resolved IR absorption bands at $15\cdot5$–$15\cdot8$ μm and $18\cdot3$–$18\cdot7$ μm. Martin (1968) gave infra-red patterns for K-feldspars synthesized hydrothermally from gels.

Fig. 8 shows data of infra-red absorption of adularia from Rhonegletscher and Seikoshi mine, together with those of the maximum microcline from the Otome mine, Japan; orthoclase ($2V_\alpha = 65°$) from Tavetsch, Switzerland, and low sanidine ($Or_{68\cdot7}Ab_{24\cdot5}An_{1\cdot5}$) from Taizi, Japan. The specimen from the Otome mine is maximum microcline without albite.

Most of the data on Disentis adularias by Hafner and Laves (1957) and on hydrothermally synthesized K-feldspars by Martin (1968) plot on the trend in fig. 8 though some data measured by Hafner and Laves deviate slightly from this trend. Judged from fig. 8, adularias from both Rhonegletscher and the Seikoshi mine are more disordered than the orthoclase from Tavetsch. The Al/Si ordering shown by IR absorption is in accordance with that indicated by observed $2V$ and

FIG. 8. Relation between two IR absorption peak wavelengths for different sectors in adularia. M: Microcline from the Otome mine, Japan. Or: Orthoclase from Tavetsch, Switzerland. R: Adularia from Rhonegletscher, Switzerland. S: Adularia from the Seikoshi mine, Japan. Sa: Sanidine from Taizi, Japan.

optical orientations. The {001} and {$\bar{1}$01} sectors in adularia from Rhonegletscher are more ordered than the {110} sector. The specimens from the Seikoshi mine are more disordered than those from Rhonegletscher, especially so their {110} sectors, which are the highest sanidine, comparable with K-feldspar synthesized hydrothermally by Martin.

The {001} and {$\bar{1}$01} sectors of adularia from both localities are optically monoclinic and the {110} sectors are triclinic. It follows from this that Al distributes differently at $Si_1(o)$ and $Si_1(m)$ sites, in spite of the fact that the structure is highly disordered so that equal distribution of Al would be expected at $Si_1(o)$ and $Si_1(m)$ sites. Therefore the {110} sector can be called triclinic disordered K-feldspar.

TRANSMISSION ELECTRON MICROSCOPY

Adularia from Rhonegletscher

The {$\bar{1}$01} sector. The inner portion consists of both fine cross-hatchings and homogeneous areas under the electron microscope. Electron-diffraction spots from the area with fine cross-hatchings exhibit cross-streaks, whereas they are sharp with no streaks in the homogeneous area. The boundary between the two areas is sharp, as can be seen in fig. 9.
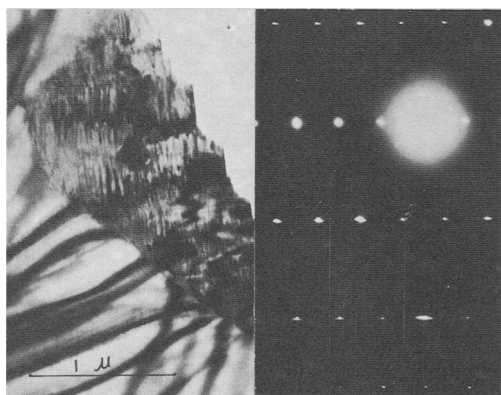
FIG. 9. Electron micrograph and electron diffraction pattern showing the coexistence of homogeneous and cross-hatched areas in adularia from Rhonegletscher. The b- and b*-axes are horizontal.

The {001} sector. Electron microscopy of the inner portion is similar to that of the {$\bar{1}$01} sector, and consists of domains showing coarse or fine cross-hatchings (fig. 10) as well as homogeneous domains.

The {110} sector. Thin foils for electron microscopic observation were prepared from the thin section normal to the c-axis. The {110} sector
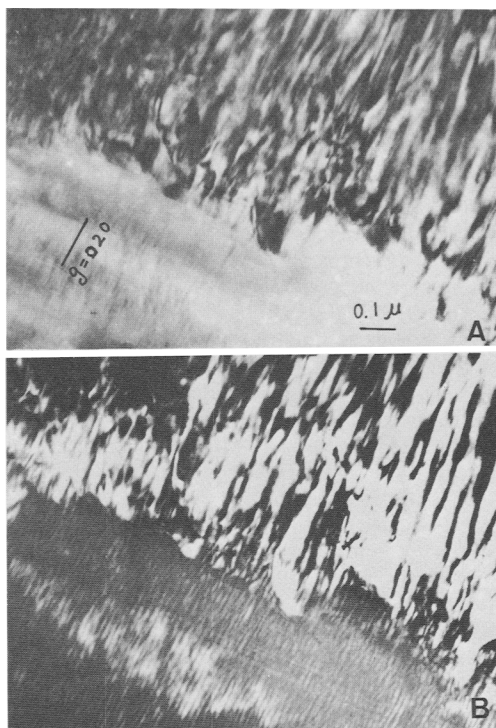

FIG. 10. Electron micrographs showing the texture of the inner part of the {110} sector. Rhonegletscher. Note the sharp boundary between coarse and fine lamellae parallel to the b-axis. A is bright field image and B dark field image due to the 020 diffraction spot.

observed under the electron microscope shows fine cross-hatchings whose fineness varies from place to place. The fine lamellae corresponding to growth bands are seen in the sector with fine cross-hatchings (fig. 11); they are not always parallel to
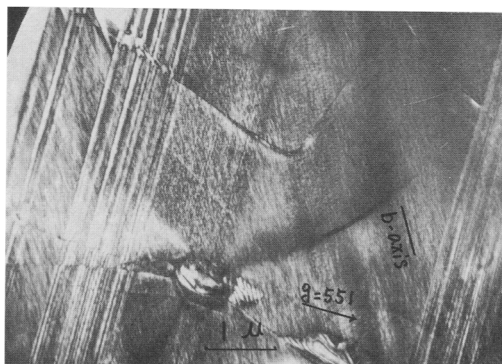

FIG. 11. Electron micrograph showing the texture of the {110} sector. Rhonegletscher. The fine growth bands parallel to the (1 10) are seen in the cross-hatched area.

(110), and when they deviate, they may be correlated with the growth bands parallel to the vicinal faces of the growth hillock. Since these lamellae become invisible when $g = hko$, the Burger's vector should be parallel to the c-axis.

Adularia from the Seikoshi mine

In general the valencianite type adularia from the Seikoshi mine shows a more homogeneous appearance or much weaker cross-hatching under the electron microscope than the Rhonegletscher specimen, though sometimes domains showing coarse cross-hatchings are found in the homogeneous area.

Many dislocations elongated in the direction roughly normal to the growth face (110) are seen in the (110) sectors with or without very fine cross-hatchings. Fig. 12 shows two types of dislocation taken under two diffraction conditions. Dislocation A, which is parallel to [130]*, is out of contrast for $g = 130$ and weak for $g = 110$. Dislocations B and C, which are roughly parallel to [110]*, are out of contrast for $g = 110$ and distinct for $g = 1\bar{1}0$. Dislocations A, B, and C are therefore of edge type. Dislocation D, which is normal to [110]*, is out of contrast and distinct for $g = 130$ and $g = 110$. It may be of screw type.
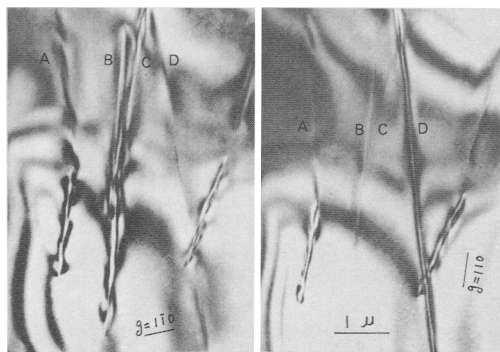

Fig. 12. Electron micrographs of dislocations in the {110} sector. Seikoshi mine. The two photographs of the same area show that the dislocations elongate in the growth direction, i.e. normal to the (110). The dislocations labelled A, B, and C are out of contrast for the 110 reflection. The dislocation labelled D is out of contrast for the $1\bar{1}0$ reflection.

DISCUSSION

In the present study, most internal textures seen optically in the thin sections correlate well with the growth patterns, for both Alpine adularia and hydrothermal valencianite. This indicates that the characteristic internal textures seen on all optical micrographs are formed during the process of

crystal growth and are well preserved throughout geologic time. There is evidence that transformation has taken place to a small extent, but such changes have not gone far enough to destroy the original textures. Bambauer and Laves concluded that adularia grew originally as monoclinic crystals and later transformed gradually to more triclinic ones with different degrees of Al/Si order, and that the characteristic internal textures of adularia are formed by the transformation process and not by growth process. They concluded this on the basis of their investigations on the thin sections prepared perpendicular to (001) and (100) or parallel to (001), (100), and (010), and not parallel to the growth faces, (110) and ($\bar{1}$01). With such sections it is difficult to make exact correlation between growth features and internal textures.

The crystals grow by piling up the many hillocks existing on the growth surface. These are from several μm to several mm in width and from several μm to about 1 mm in thickness. As the optical properties are different from domain to domain made by crystal growth on vicinal faces of the hillocks, growth features can be seen in the thin section of the inner portion of the crystal under the polarizing microscope. A thin section that is not parallel to the growth plane shows the growth lamellae as seen in fig. 4, and a thin section parallel to the growth plane shows growth domains similar to growth hillocks on the surface as seen in figs. 1, 2, and 6, so that the correlation between growth features and internal texture is difficult with the former and easy with the latter. Also, Bambauer and Laves did not consider the rim of adularia from Switzerland, at which a one-to-one correlation can be seen easily under the polarized microscope.

The cross-hatching that is formed in the process of phase transition is not evident in our transmission electron microscope work, except very faintly in some areas of the crystal from the Seikoshi mine, and is found coexisting with more or less homogeneous areas in the crystals from Rhonegletscher. From these, it is safe to conclude that the valencianite crystals from the Seikoshi mine have not experienced severe transition since they were formed, and that adularia crystals from Rhonegletscher have experienced transition to some extent, but not so much as to destroy the original textures.

Now, on the basis of the above, let us consider the variation in optics of these crystals. Since adularia (valencianite, too) grew under non-equilibrium conditions, it is possible for changes of the ordering of Al/Si to occur during crystal growth, by two mechanisms:

Growth speed. The higher the growth speeds, the more disordered the phase. A possibility of the

effect of growth speed upon the optics was suggested by Laves (1952), who mentioned that the rate of growth is high enough so that the ordering force is overwhelmed during crystallization, thus forming a more or less disordered $AlSi_3O_8$ framework.

The area grown parallel to stable growth planes such as (110), (001), and (10̄1) will be more disordered than the areas grown on the side vicinal faces of growth hillocks on the same crystal face, since the rate of advance of growth layers is highest along the stable face, and slower for those of bunched growth layers forming side vicinal faces. This is so in the case of the (1̄10) face of valencianite from the Seikoshi mine as can be seen in fig. 7.

It is also seen in figs. 4 and 5 that the structure is more ordered in the later-formed parts of the crystals. This is attributed to the fact that the growth speed on the (10̄1) face is high at the initial stage, and diminishes later. If growth layers advance at constant rate, the same ordering of Al/Si in a monoclinic or triclinic structure can be expected, which will result in an optically homogeneous crystal. The internal homogeneous portion seen in Rhonegletscher specimens must have been formed in such a manner.

Now, let us compare the optics of the {110} sector of adularia from Rhonegletscher and of valencianite from the Seikoshi mine (fig. 7) as well as the optics of adularia from Val Casatscha, Switzerland, measured by Bambauer and Laves (1960). The 2V values decrease in the order of Rhonegletscher, Val Casatscha, and the Seikoshi mine when the optic plane is ∥ (010), and increase in the same order when it is ⊥ (010). Although the two curves for valencianite from the Seikoshi mine and adularia from Val Casatscha have similar trends, the former shows higher 2V values on the high sanidine side, i.e. highest sanidine optics, and such optics were not found on the latter specimen. Many domains of valencianite from the Seikoshi mine show the optics of high sanidine side (optic plane ∥ (010)), and many domains of adularia from Rhonegletscher, especially {001} and {10̄1} sectors, show the optics of microcline (optic plane approximately ⊥ (010)). These results show that the degree of Al/Si ordering of the two adularias from the Swiss Alps is greater on the average than for valencianite from the Seikoshi mine, the Rhonegletscher specimens being the most ordered.

Difference of the two-dimensional atomic arrangement on growth surfaces. The difference of the atomic arrangement exposed on the (110), (10̄1), and (001) surfaces will affect the ordering in non-equilibrium growth conditions. Irrespective of growth speeds and degree of order, the symmetry of each sector is maintained. The {110} sector is triclinic; {001}, {10̄1} sectors are monoclinic.

To explain the above the structure of monoclinic feldspar is projected parallel to (001) as shown in fig. 13. In monoclinic disordered K-feldspar, i.e. sanidine, Al distributes equally at the two sites $Si_1(o)$ and $Si_1(m)$, whereas the two sites are not equivalent in a triclinic crystal. In fig. 13, one $Si_1(m)$ and two Si_2 sites are on the same sheet parallel to the (110), and $Si_1(o)$ sites join the neighbouring two sheets. Contrariwise, $Si_1(o)$ and two Si_2 sites are on the same sheet parallel to the (1̄10) plane, and $Si_1(m)$ sites join the neighbouring two sheets. The $Si_1(o)$ and $Si_1(m)$ sites are thus not equivalent on the (110) and (1̄10) planes.

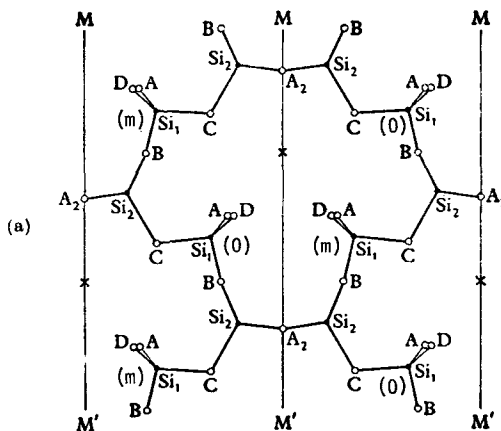
FIG. 13. Atomic structure of monoclinic potash feldspar viewed normal to (001) (modified from Deer *et al.*, 1963).

In contrast, $Si_1(o)$ and $Si_1(m)$ sites in the (001) and (10̄1) planes that are on the same plane parallel to the *b*-axis are equivalent, as can be seen in fig. 13. It follows from this that the (110) and (1̄10) sectors should become triclinic, the (001) and (10̄1) sectors monoclinic.

Finally, it should be emphasized that unless adularia grows under non-equilibrium conditions, these characteristics, i.e. sector textures, their optics, their ordering states, and monoclinic (001), (10̄1) sectors and triclinic (110), (1̄10) sectors, will not be formed. If it had grown under equilibrium conditions, the crystal should be maximum microcline since this is the assumed stable form at low temperatures.

REFERENCES

Akizuki (M.) and Sunagawa (I.), 1975. *Sci. Report, Tohoku Univ.*, Series III, **13**, 67.

Ansilewski (J.), 1961. *Bull. Acad. Polon. Sci. Chem. Geol. Geogr.* **6**, 275.

Bambauer (H. U.) and Laves (F.), 1960. *Schweiz. Mineral. Petrogr. Mitt.* **40**, 177.

Barth (R. F. W.), 1928. *Z. Kristallogr.* **68**, 473.

—— 1929. *Fortschr. Mineral.* **13-14**, 185.

Chaisson (U.), 1950. *J. Geol.* **58**, 537.

Deer (W. A.), Howie (R. A.), and Zussman (J.), 1963. *Rock Forming Minerals*, **4**. Longmans.

Hafner (S.) and Laves (F.), 1957. *Z. Kristallogr.* **109**, 204.

Köhler (A.), 1949. *Neues Jahrb. Mineral.* 1945–8, *Abt. A, Monatsch.* 49.

Laves (F.), 1950. *J. Geol.* **58**, 548.

—— 1952. Ibid. **60**, 436.

Mallard (F.), 1876. *Ann. Mines.* **10**, 187.

Martin (R. F.), 1968. Ph.D. Thesis, Stanford University.

McConnell (J. D. C.), 1965. *Philos. Mag.* **11**, 1289.

Steiner (A.), 1970. *Mineral. Mag.* **37**, 916.